

# Probing Light Dark Matter through Cosmic-Ray Cooling in Active Galactic Nuclei

Gonzalo Herrera<sup>1,2</sup>, Kohta Murase<sup>3,4,5</sup>

<sup>1</sup>Physik-Department, Technische Universität München,  
James-Frank-Straße, 85748 Garching, Germany,

<sup>2</sup>Max-Planck-Institut für Physik (Werner-Heisenberg-Institut), Föhringer Ring 6, 80805 München, Germany,

<sup>3</sup>Department of Physics; Department of Astronomy & Astrophysics; Center for Multimessenger Astrophysics,  
Institute for Gravitation and the Cosmos, The Pennsylvania State University, University Park, PA 16802, USA,

<sup>4</sup>School of Natural Sciences, Institute for Advanced Study, Princeton, NJ 08540, USA,

<sup>5</sup>Center for Gravitational Physics and Quantum Information,

Yukawa Institute for Theoretical Physics, Kyoto University, Kyoto, Kyoto 606-8502, Japan

Recent observations of high-energy neutrinos from active galactic nuclei (AGN), NGC 1068 and TXS 0506+056, suggest that cosmic rays (CRs) are accelerated in the vicinity of the central supermassive black hole and high-energy protons and electrons can cool efficiently via interactions with ambient photons and gas. The dark matter density may be significantly enhanced near the black hole, and CRs could lose energies predominantly due to scatterings with the ambient dark matter particles. We propose CR cooling in AGN as a new probe of dark matter-proton and dark matter-electron scatterings. Under plausible astrophysical assumptions, our constraints on sub-GeV dark matter can be the strongest derived to date. Some of the parameter space favored by thermal light dark matter models might already be probed with current multimessenger observations of AGN.

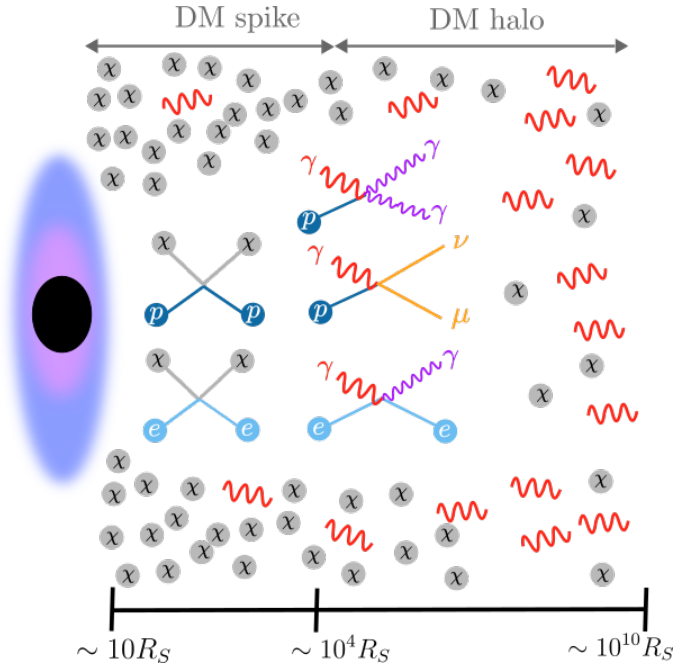


FIG. 1. Schematic picture of dark cooling of CRs due to elastic scatterings with dark matter particles in AGN. High-energy protons and electrons may traverse a high density of dark matter particles more efficiently than standard cooling processes involving neutrino and photon emission.

## INTRODUCTION

The presence of dark matter in galaxies and clusters of galaxies is well established by astrophysical and cosmological observations [1]. However, its particle nature remains unknown [2]. A variety of experiments have aimed to detect dark matter particles via their scatter-

ings off nuclei and/or electrons at Earth-based detectors, setting strong upper limits on the interaction strength of dark matter particles with masses in the GeV-TeV scale, but leaving the sub-GeV region of the parameter space yet largely unconstrained [3–7]. Historically, dark matter fermions with sub-GeV masses were disfavoured by the cosmological bound [8, 9]. However, large parameter space still remains unexplored in more complicated but well-motivated scenarios [10–12].

Different approaches have been proposed to extend the sensitivity reach of direct detection experiments for sub-GeV dark matter masses. Some of these consider a boosted component of dark matter particles reaching the Earth, purely via gravitational effects (*e.g.*, Refs. [13–18]), while others rely on a boosted component due to scatterings of dark matter particles with protons or electrons in different astrophysical environments (*e.g.*, Refs. [19–28]).

Active galactic nuclei (AGN) are promising sources of high-energy protons and electrons. While the dominant acceleration mechanism of these cosmic rays (CRs) is still under debate, modeling of multimessenger data have placed important constraints on not only energetics of CR production but also the emission region of the observed neutrinos that can be produced either via inelastic  $pp$  collisions or  $p\gamma$  interactions [29–31]. For example, observations of high-energy neutrinos and gamma rays from NGC 1068 [32, 33] suggest that the neutrino production occurs in the vicinity of the supermassive black hole (SMBH) at  $R_{\text{em}} \lesssim 30 - 100 R_S$  (where  $R_S$  is the Schwarzschild radius), which is consistent with theoretical models [34–38], and the required proton luminosity is at least  $\sim 10\%$  of the intrinsic X-ray luminosity [39, 40]. Another neutrino source candidate, TXS 0506+056 [41–45], is known to be a jet-loud AGN, and

	$R_{\text{em}}$	$M_{\text{BH}}$	$t_{\text{BH}}$	$r_0$	$\langle\sigma v\rangle/m_{\text{DM}}$	$\langle\rho_{\text{DM}}\rangle$
NGC 1068 (I)	$30 R_S$	$(1-2) \times 10^7 M_\odot$	$10^{10}$ yr	10 kpc	0	$7 \times 10^{17}$ GeV/cm <sup>3</sup>
NGC 1068 (II)	$30 R_S$	$(1-2) \times 10^7 M_\odot$	$10^{10}$ yr	10 kpc	$10^{-31}$ cm <sup>3</sup> s <sup>-1</sup> /GeV	$4 \times 10^{13}$ GeV/cm <sup>3</sup>
TXS 0506+056 (I)	$10^4 R_S$	$(3-10) \times 10^8 M_\odot$	$10^9$ yr	10 kpc	0	$8 \times 10^{12}$ GeV/cm <sup>3</sup>
TXS 0506+056 (II)	$10^4 R_S$	$(3-10) \times 10^8 M_\odot$	$10^9$ yr	10 kpc	$10^{-28}$ cm <sup>3</sup> s <sup>-1</sup> /GeV	$4 \times 10^{11}$ GeV/cm <sup>3</sup>

TABLE I. Relevant parameters considered in this work for NGC 1068 and TXS 0506+056, for two different sets of assumptions dubbed (I) and (II). Here  $R_{\text{em}}$  represents the distance of the emission region from the central SMBH in NGC 1068 (TXS 0506+056),  $M_{\text{BH}}$  shows the SMBH mass and its uncertainty,  $t_{\text{BH}}$  is the age elapsed since the black hole was formed,  $r_0$  is the scale radius of the galaxy,  $\langle\sigma v\rangle/m_{\text{DM}}$  denotes the assumed values of the effective dark matter self-annihilation cross section, and  $\langle\rho_{\text{DM}}\rangle$  is the average density of dark matter particles within  $R_{\text{em}}$ .

the observed spectral energy distribution in photons is mostly explained by synchrotron and inverse-Compton emission from CR electrons [44, 46–50], and the proton luminosity required by IceCube observations may even exceed the Eddington luminosity [46, 47].

In this work, we propose CRs produced in AGN as a new probe of dark matter-proton and dark matter-electron scatterings through their multimessenger observations. Given that emission regions of neutrinos and gamma rays are constrained to be near the SMBHs, CRs also need to traverse the dark matter spike around the central SMBH. If such additional cooling beyond the standard model (BSM) was too strong, CR energy losses are modified so that the required CR luminosity would be larger, and the neutrino and photon spectra could even be incompatible with the observations. Our work is different from previous studies on AGN probes of the dark matter scatterings with protons and electrons, which focused either on the boosted flux of dark matter particles from the source at Earth [22, 51, 52], or on the spectral distortions in the gamma-ray flux induced by CR scatterings off dark matter particles [53–57]. Instead we focus on the impact of the dark matter-proton and dark matter-electron scatterings on the neutrino and photon fluxes or the CR power, considering for the first time the cooling of protons and electrons in the inner regions of the AGN, where a dark matter spike is likely to be formed.

## DARK MATTER DISTRIBUTION IN AGN

The adiabatic growth of black holes may form a spike of dark matter particles in their vicinity [58–61]. An initial dark matter profile of the form  $\rho(r) = \rho_0(r/r_0)^{-\gamma}$  evolves into:

$$\rho_{\text{sp}}(r) = \rho_R g_\gamma(r) \left(\frac{R_{\text{sp}}}{r}\right)^{\gamma_{\text{sp}}}, \quad (1)$$

where  $R_{\text{sp}} = \alpha_\gamma r_0 (M_{\text{BH}}/(\rho_0 r_0^3))^{\frac{1}{3-\gamma}}$  is the size of the spike, with  $\alpha_\gamma \simeq 0.293\gamma^{4/9}$  for  $\gamma \ll 1$ , and numerical values for other values of  $\gamma$  are provided in Ref. [60]. The cuspleness of the spike is given by  $\gamma_{\text{sp}} = \frac{9-2\gamma}{4-\gamma}$ . Further,  $g_\gamma(r)$  can be approximated for  $0 < \gamma < 2$  by

$g_\gamma(r) \approx (1 - \frac{4R_S}{r})$ , while  $\rho_R$  is a normalization factor, chosen to match the density profile outside of the spike,  $\rho_R = \rho_0 (R_{\text{sp}}/r_0)^{-\gamma}$ . This density profile vanishes at  $4R_S$ , which is, however, a conservative approximation that neglects relativistic and rotation effects in black holes [62, 63].

We consider that the initial dark matter distribution follows an Navarro-Frenk-White (NFW) profile [64, 65], with  $\gamma = 1$ , resulting in a spike with  $\gamma_{\text{sp}} = 7/3$  and  $\alpha_\gamma = 0.122$ . The masses of the central SMBHs of the two AGN considered in this work are given in Table I. For the scale radius of both galaxies, we take  $r_0 = 10$  kpc. Finally, the normalization  $\rho_0$  is determined by the uncertainty on the black hole mass [54, 66], also provided in Table I. We have checked that this criteria yields masses of the dark matter halo compatible with those expected from universal relations between SMBH and galaxy masses [67, 68].

This profile only holds when the dark matter particles do not effectively self-annihilate, or self-annihilate very slowly (*e.g.*, as in scenarios of asymmetric dark matter or axions). If they self-annihilate with a sufficiently large cross section, the maximal dark matter density in the inner regions of the spike is saturated to  $\rho_{\text{sat}} = m_{\text{DM}}/(\langle\sigma v\rangle t_{\text{BH}})$ , where  $\langle\sigma v\rangle$  is the velocity averaged dark matter self-annihilation cross section, and  $t_{\text{BH}}$  is the time passed since the black hole was formed. For TXS 0506+056, we take the value  $t_{\text{BH}} = 10^9$  yr [51], while for NGC 1068 we use  $t_{\text{BH}} = 10^{10}$  yr [69]. Furthermore, the dark matter spike extends to a maximal radius  $R_{\text{sp}}$ , beyond which the dark matter distribution follows the initial NFW profile. The dark matter density profile therefore reads [60, 66, 70]

$$\rho(r) = \begin{cases} 0 & r \leq 4R_S, \\ \frac{\rho_{\text{sp}}(r)\rho_{\text{sat}}}{\rho_{\text{sp}}(r)+\rho_{\text{sat}}} & 4R_S \leq r \leq R_{\text{sp}}, \\ \rho_0 \left(\frac{r}{r_0}\right)^{-\gamma} \left(1 + \frac{r}{r_0}\right)^{-(3-\gamma)} & r \geq R_{\text{sp}}. \end{cases} \quad (2)$$

The dark matter profiles in TXS 0506+056 and NGC 1068 are shown in the left panel of Fig. 2 for two values of  $\langle\sigma v\rangle/m_{\text{DM}}$  allowed for sub-GeV dark matter [71–73].

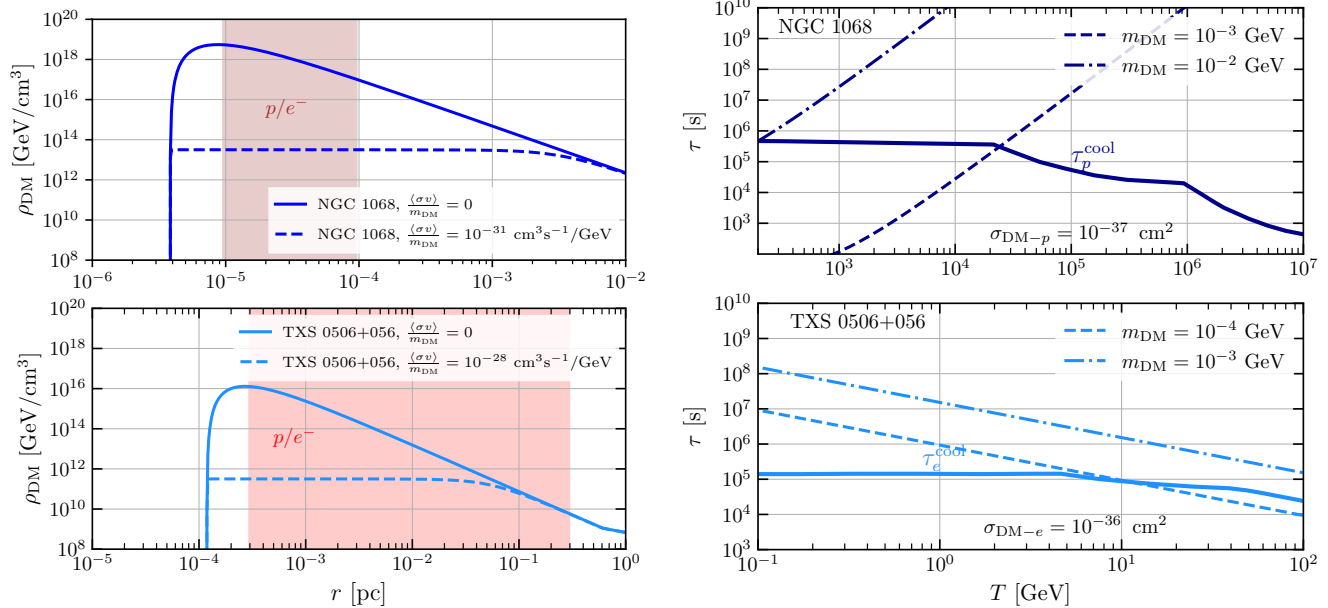


FIG. 2. *Left panel:* Dark matter distribution around the SMBHs of TXS 0506+056 and NGC 1068, for different values of the dark matter self-annihilation cross section over its mass. The red (brown) shaded region indicates the region where the production of high-energy particles is expected to take place in TXS 0506+056 (NGC 1068). *Right panel:* In solid lines, we show the cooling time scales of protons (electrons) in NGC 1068 (TXS 0506+056) (see main text for details). In dashed and dot-dashed lines we show the time scales due to elastic dark matter proton and dark matter-electron scatterings, for different values of the dark matter mass and scattering cross section.

We find that the dark matter density is extremely high in the region where high-energy particles are produced, and dark interactions with dark matter particles may lead to a sizable depletion of the observed fluxes.

### BSM COOLING OF CRS IN AGN

Neutrinos and photons from AGN can be explained by emission from high-energy protons and electrons through purely Standard Model mechanisms. Energy-loss mechanisms include scatterings with other Standard Model particles in the plasma or synchrotron radiation as well as adiabatic losses. In addition, there are escape losses due to advection or diffusion via magnetic fields. The presence of dark matter coupling to protons and electrons in the vicinity of SMBHs would naturally introduce additional scattering time scales, leading to the suppression of the observed neutrino and gamma-ray fluxes in certain energy ranges, if the BSM cooling time scales of CRS were shorter than the standard cooling time scales. For example, at  $m_{\text{DM}} \sim 10^{-3}$  GeV, the currently-allowed maximum dark matter-proton scattering cross section stems from blazar-boosted dark matter, with a value of  $\sigma_{\text{DM-p}} \sim 10^{-33}$  cm<sup>2</sup>. As discussed in the previous section, the average density of (asymmetric) dark matter particles in the coronal region of NGC 1068 is  $\langle\rho_{\text{DM}}\rangle \sim 10^{18}$  GeV/cm<sup>3</sup>. Thus, if the corresponding cross

section for CR protons is comparable to  $\sigma_{\text{DM-p}}$  (although this is not the case in general), the BSM cooling time scale for the currently allowed values in the literature is  $\tau_{\text{DM-p}} \sim 1/(\langle n_{\text{DM}} \rangle \sigma_{\text{DM-p}} c) \sim 30$  s, which is well below the proton cooling time inferred by observations of NGC 1068. This simple estimate clearly suggests that CRs in AGN can provide a powerful probe of these interactions.

More quantitatively, the BSM cooling time scale due to elastic dark matter scattering off CRS is given by [57]

$$\tau_{\text{DM-i}}^{\text{el}} = \left[ -\frac{1}{E} \left( \frac{dE}{dt} \right)_{\text{DM-i}} \right]^{-1}, \quad (3)$$

with

$$\left( \frac{dE}{dt} \right)_{\text{DM-i}} = -\frac{\langle\rho_{\text{DM}}\rangle}{m_{\text{DM}}} \int_0^{T_{\text{DM}}^{\text{max}}} dT_{\text{DM}} T_{\text{DM}} \frac{d\sigma_{\text{DM-CR}i}}{dT_{\text{DM}}}, \quad (4)$$

where  $\langle\rho_{\text{DM}}\rangle$  is the average density of dark matter particles in the region of CR production. See Table I for the specific values that we use for NGC 1068 and TXS 0506+056. Also,  $d\sigma_{\text{DM-CR}i}/dT_{\text{DM}}$  is the differential elastic dark matter-proton or dark matter-electron cross section,  $T_{\text{DM}}^{\text{max}}$  is the maximal allowed value for  $T_{\text{DM}}$  in a collision with a particle  $i$  with kinetic energy  $T = E - m_i$ , which is

$$T_{\text{DM}}^{\text{max}} = \frac{2T^2 + 2m_i T}{m_{\text{DM}}} \left[ \left( 1 + \frac{m_i}{m_{\text{DM}}} \right)^2 + \frac{2T}{m_{\text{DM}}} \right]^{-1}. \quad (5)$$

We consider fermionic dark matter which elastically interacts with protons and electrons via a heavy scalar mediator. The differential cross section reads [74]

$$\frac{d\sigma_{\text{DM-CR}i}}{dT_{\text{DM}}} = \frac{\sigma_{\text{DM-}i}}{T_{\text{DM}}^{\text{max}}} \frac{F_i^2(q^2)}{16\mu_{\text{DM-}i}^2 s} (q^2 + 4m_i^2)(q^2 + 4m_{\text{DM}}^2), \quad (6)$$

where  $\sigma_{\text{DM-}i}$  is the dark matter-proton or dark matter-electron cross section at the zero center-of-mass momentum,  $\mu_{\text{DM-}i}$  is the reduced mass,  $s$  is the square of center-of-mass energy, and  $q^2 = 2m_{\text{DM}}T_{\text{DM}}$  is the momentum transfer of the process. The quantity  $F_i$  is either the proton form factor [75], or equal to 1 for electrons. This formalism is only valid for elastic scatterings.

In the right panel of Fig. 2, the solid lines represent the total standard energy-loss time scales as a function of energy for protons in NGC 1068 [39] and for electrons in TXS 0506+056 [76]. CR protons in NGC 1068 are almost depleted, and the dominant cooling mechanisms at increasing energies are inelastic  $pp$  interactions, Bethe-Heitler pair production, and  $p\gamma$  interactions [34]. CR protons do not cool efficiently in TXS 0506+056, and the fate is governed by a dynamical time scale of  $\sim 10^5$  s in the SMBH frame [76]. For electrons in TXS 0506+056, the dominant cooling mechanisms are inverse Compton scattering and synchrotron radiation. The breaks in the solid lines of the plots reflect the energies at which the transition of dominant processes occurs.

For comparison, we also show BSM cooling time scales due to elastic dark matter scatterings with protons and electrons. The dotted-dashed line corresponds to values of the dark matter mass and cross section that would induce a contribution smaller than the proton and electron energy losses due to the Standard Model processes. On the other hand, the dashed line shows values of the parameters that would induce larger energy losses than in the Standard Model at relevant energies (according to our exclusion limit criterion). It is important to point out that inelastic dark matter-proton scatterings are expected to dominate over the elastic channel at energies  $E \gtrsim m_p^2/2m_{\text{DM}}$ , however, the inelastic cross section is sensitive to the details of the dark matter particle model, therefore we decide to restrict our analysis to the elastic scattering channel. Including inelastic channels would probably allow to derive stronger limits, although one should then consider the production of additional neutrinos and photons via pion decay, as done in Refs. [55, 57].

For the purpose of constraining the interaction strength, we find for each  $m_{\text{DM}}$  the largest dark matter-proton (electron) scattering cross section yielding a time scale equal or larger to the cooling time scales determined with models at relevant energies. In particular, we use

$$\tau_{\text{DM-}i}^{\text{el}} \geq C \tau_i^{\text{cool}}. \quad (7)$$

The coefficient  $C$  is a model dependent factor, and we use  $C = 0.1$  in this work. In other words, we find the

maximum dark matter-proton (electron) scattering cross section that would have an  $\mathcal{O}(10)$  or less impact on the proton (electron) cooling time scale. This is reasonable and may be even conservative from the energetics requirement of neutrino-emitting AGN. For NGC 1068, the proton luminosity would be  $10^{43} \text{ erg s}^{-1} \lesssim L_p \lesssim L_X \lesssim 10^{44} \text{ erg s}^{-1}$  [34, 39], justifying  $C \sim 0.1 - 1$ . For TXS 0506+056, the proton luminosity in the single-zone model already violates the Eddington luminosity  $L_{\text{Edd}}$  [46], so our choice is conservative. This is also reasonable for electrons because of  $L_e \sim 8 \times 10^{47} \text{ erg s}^{-1} \sim 20L_{\text{Edd}}$  [76]. In principle, if the CR acceleration mechanism is understood, spectral modification due to BSM cooling may allow us to improve constraints and  $C \sim 1$  is possible. For proton energies of interest, because neutrinos carry  $\sim 5\%$  of the proton energy, we use 30–300 TeV for NGC 1068 [32] and 0.2–20 PeV for TXS 0506+056 [42], which lead to conservative constraints. For electrons, we use 50 GeV – 2 TeV following Ref. [76].

Applying the condition of Eq. (7) for NGC 1068 and TXS 0506+056, we set constraints on the spin-independent dark matter-proton and dark matter-electron scattering cross sections via a heavy mediator (see Fig. 3). The solid lines correspond to scenario (I), and the dashed lines correspond to scenario (II) (see Table I), corresponding to different values of the dark matter self-annihilation cross section consistent with current constraints [73]. When the dark matter self-annihilates, the dark matter spike is saturated near the SMBH, and the average density of dark matter particles in the region where CRs are confined is smaller. We find that our constraints become stronger at lower dark matter masses. This is mainly due to the fact that the number density of dark matter particles increases with decreasing masses, and the cross section needed to induce large energy losses becomes smaller. However, we note that for protons the dependence of the constraint on the dark matter mass is more pronounced than for electrons. This is because we only consider elastic scatterings accounting for energy losses, and the elastic scattering cross section decreases with reference to its maximum value for  $E \gtrsim m_p^2/2m_{\text{DM}}$ .

For comparison, we show complementary constraints from other methods. The green region is excluded by dark matter direct detection experiments [77–80], where the maximal cross section unaffected by atmospheric scatterings is considered [81, 82]. The magenta region is constrained by the X-ray Quantum Calorimeter (XQC) experiment [83]. The cyan region is constrained by Milky Way satellite galaxy counts [84], and the grey region is constrained by the Big Bang nucleosynthesis (BBN) [85, 86]. Finally, the orange region is constrained by CR boosted dark matter (CRBDM) at XENON1T [19], and the red regions are excluded when considering the blazar-boosted dark matter flux from TXS 0506+056 [22, 51]. Further, for dark matter-electron scatterings, we include constraints from the solar reflection [87], and the region of

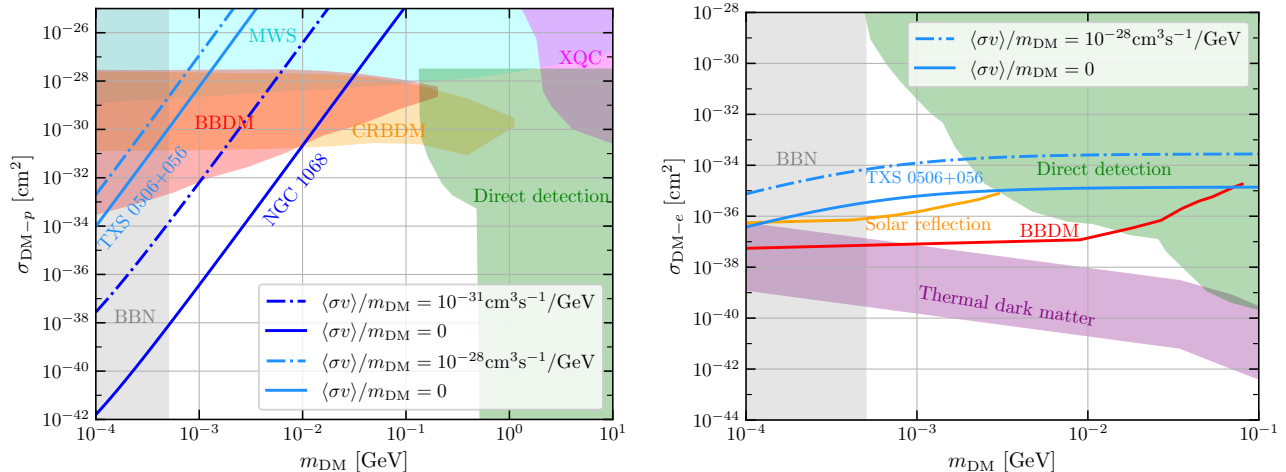


FIG. 3. *Left panel:* Upper limits on the spin-independent dark matter-proton scattering cross-section as a function of the dark matter mass, derived from the requirement that the required proton luminosity is substantially larger due to scatterings off dark matter particles in NGC 1068 and TXS 0506+056. The different blue shadings correspond to two different assumptions on the dark matter self-annihilation cross section, which affects the average density of dark matter particles in the inner regions of the AGN. Complementary constraints from different searches are shown for comparison (see main text for details). *Right panel:* Analogous upper limits on the dark matter-electron scattering cross section, for TXS 0506+056. We also display values of the dark matter-electron scattering cross section vs dark matter mass compatible with thermal production of light dark matter. Note that we do not have constraints from NGC 1068 because the observed gamma rays may be purely hadronic [33].

values where light thermal dark matter acquires its relic abundance via various mechanisms [12, 88, 89]. From Fig. 3, one sees that our constraints for asymmetric (self-annihilating) light dark matter coupling to protons are stronger than complementary bounds for  $m_{\text{DM}} \lesssim 10^{-2}$  GeV ( $m_{\text{DM}} \lesssim 10^{-3}$  GeV). For dark matter-electron scatterings, our constraints are stronger than direct detection bounds at masses below  $m_{\text{DM}} \lesssim 5 \times 10^{-3}$  GeV. In addition, for dark matter-electron interactions, AGN data allows to probe the parameter space favored for dark matter models with  $m_{\text{DM}} \lesssim 10^{-4}$  GeV, although this region might be in conflict with BBN. Effects of different assumptions on the dark matter distribution are discussed in the Supplementary Material.

## SUMMARY AND DISCUSSION

Recent multimessenger measurements of AGN have indicated that high-energy particles, in particular CR protons and secondary neutrinos, are produced in the vicinity of SMBHs. CR cooling could be significantly enhanced by BSM interactions with dark matter, thanks to the formation of a dark matter spike around the central SMBH, with a large density. We demonstrated that neutrino-emitting AGN, NGC 1068 and TXS 0506+056, allow us to set strong constraints on sub-GeV dark matter coupled to protons and/or electrons.

Our constraints on asymmetric (self-annihilating) light dark matter coupling to protons are stronger than other

complementary bounds for  $m_{\text{DM}} \lesssim 10^{-2}$  GeV ( $m_{\text{DM}} \lesssim 10^{-3}$  GeV). For dark matter-electron scatterings, our constraints are stronger than direct detection bounds at masses below  $m_{\text{DM}} \lesssim 5 \times 10^{-3}$  GeV, which potentially allows us to probe the parameter space favored for thermal dark matter models with  $m_{\text{DM}} \lesssim 10^{-4}$  GeV.

The current constraints are subject to uncertainties from the dark matter distribution in the inner regions of AGN as well as on CR cooling time scales. Nevertheless, for the latter, we stress that our constraints are rather conservative especially for NGC 1068. This is because the source has to be nearly calorimetric to explain the neutrino flux [39], and relaxing assumptions (*e.g.*, with softer CR spectra) will make the limits stronger. Future multimessenger observations and astrophysical modeling will allow us to better understand the sources and reduce uncertainties, and the resulting limits on the dark matter-proton and the dark matter-electron cross section will become more stringent and robust. Understanding acceleration mechanisms will also enable us to compare  $\tau_{\text{DM}-i}^{\text{el}}$  to the acceleration time scale for placing constraints.

Multimessenger observations of neutrino sources have been proposed to study dark matter interactions with photons [63] and neutrinos [63, 90–97], as well as historically-investigated annihilating or decaying signatures. Now there is accumulating evidence that AGN can accelerate CRs to TeV–PeV energies. We demonstrate that high-energy particle emission from AGN provides us with a powerful probe of dark matter scatterings with protons and electrons.

## ACKNOWLEDGEMENTS

We are very grateful to Francesca Capel, Mar Císcar, Francesc Ferrer, Alejandro Ibarra, Walter Winter, Chengchao Yuan, and Bing Zhang for useful discussions. KM thanks the Topical Workshop: NGC 1068 as cosmic laboratory sponsored by SFB1258 and Cluster of Excellence ORIGINS. GH is supported by the Collaborative Research Center SFB1258 and by the Deutsche Forschungsgemeinschaft (DFG, German Research Foundation) under Germany's Excellence Strategy - EXC-2094 - 390783311. KM is supported by the NSF Grant No. AST-1908689, No. AST-2108466 and No. AST-2108467, and KAKENHI No. 20H01901 and No. 20H05852.

- 
- [1] G. Bertone and D. Hooper, *Rev. Mod. Phys.* **90**, 045002 (2018), arXiv:1605.04909 [astro-ph.CO].
- [2] G. Bertone, D. Hooper, and J. Silk, *Phys. Rept.* **405**, 279 (2005), arXiv:hep-ph/0404175.
- [3] M. W. Goodman and E. Witten, *Phys. Rev. D* **31**, 3059 (1985).
- [4] R. Bernabei *et al.*, *Phys. Rev. D* **77**, 023506 (2008), arXiv:0712.0562 [astro-ph].
- [5] T. Marrodán Undagoitia and L. Rauch, *J. Phys. G* **43**, 013001 (2016), arXiv:1509.08767 [physics.ins-det].
- [6] R. Essig, J. Mardon, and T. Volansky, *Physical Review D* **85** (2012), 10.1103/physrevd.85.076007.
- [7] R. Essig, G. K. Giovanetti, N. Kurinsky, D. McKinsey, K. Ramanathan, K. Stifter, and T.-T. Yu, in *2022 Snowmass Summer Study* (2022) arXiv:2203.08297 [hep-ph].
- [8] P. Hut, *Physics Letters B* **69**, 85 (1977).
- [9] B. W. Lee and S. Weinberg, *Phys. Rev. Lett.* **39**, 165 (1977).
- [10] C. Boehm and P. Fayet, *Nucl. Phys. B* **683**, 219 (2004), arXiv:hep-ph/0305261.
- [11] L. J. Hall, K. Jedamzik, J. March-Russell, and S. M. West, *JHEP* **03**, 080 (2010), arXiv:0911.1120 [hep-ph].
- [12] Y. Hochberg, E. Kuflik, T. Volansky, and J. G. Wacker, *Phys. Rev. Lett.* **113**, 171301 (2014), arXiv:1402.5143 [hep-ph].
- [13] A. N. Baushev, *Astrophys. J.* **771**, 117 (2013), arXiv:1208.0392 [astro-ph.CO].
- [14] P. S. Behroozi, A. Loeb, and R. H. Wechsler, *Journal of Cosmology and Astroparticle Physics* **2013**, 019 (2013).
- [15] G. Besla, A. Peter, and N. Garavito-Camargo, *JCAP* **11**, 013 (2019), arXiv:1909.04140 [astro-ph.GA].
- [16] G. Herrera and A. Ibarra, *Phys. Lett. B* **820**, 136551 (2021), arXiv:2104.04445 [hep-ph].
- [17] G. Herrera, A. Ibarra, and S. Shirai, *JCAP* **04**, 026 (2023), arXiv:2301.00870 [hep-ph].
- [18] A. Smith-Orlik *et al.*, (2023), arXiv:2302.04281 [astro-ph.GA].
- [19] T. Bringmann and M. Pospelov, *Phys. Rev. Lett.* **122**, 171801 (2019), arXiv:1810.10543 [hep-ph].
- [20] Y. Ema, F. Sala, and R. Sato, *Phys. Rev. Lett.* **122**, 181802 (2019), arXiv:1811.00520 [hep-ph].
- [21] J. Alvey, M. Campos, M. Fairbairn, and T. You, *Phys. Rev. Lett.* **123**, 261802 (2019), arXiv:1905.05776 [hep-ph].
- [22] J.-W. Wang, A. Granelli, and P. Ullio, (2021), arXiv:2111.13644 [astro-ph.HE].
- [23] K. Agashe, Y. Cui, L. Necib, and J. Thaler, *JCAP* **10**, 062 (2014), arXiv:1405.7370 [hep-ph].
- [24] D. Kim, J.-C. Park, and S. Shin, *Phys. Rev. Lett.* **119**, 161801 (2017), arXiv:1612.06867 [hep-ph].
- [25] A. Das and M. Sen, *Phys. Rev. D* **104**, 075029 (2021), arXiv:2104.00027 [hep-ph].
- [26] C. V. Cappiello, N. P. A. Kozar, and A. C. Vincent, *Phys. Rev. D* **107**, 035003 (2023), arXiv:2210.09448 [hep-ph].
- [27] C. A. Argüelles, V. Muñoz, I. M. Shoemaker, and V. Takhstov, *Phys. Lett. B* **833**, 137363 (2022), arXiv:2203.12630 [hep-ph].
- [28] Y.-H. Lin, W.-H. Wu, M.-R. Wu, and H. T.-K. Wong, *Phys. Rev. Lett.* **130**, 111002 (2023), arXiv:2206.06864 [hep-ph].
- [29] K. Murase, M. Ahlers, and B. C. Lacki, *Phys. Rev. D* **88**, 121301 (2013), arXiv:1306.3417 [astro-ph.HE].
- [30] W. Winter, *Phys. Rev. D* **88**, 083007 (2013), arXiv:1307.2793 [astro-ph.HE].
- [31] K. Murase, D. Guetta, and M. Ahlers, *Physical Review Letters* **116** (2016), 10.1103/physrevlett.116.071101.
- [32] R. Abbasi *et al.* (IceCube), *Science* **378**, 538 (2022), arXiv:2211.09972 [astro-ph.HE].
- [33] M. Ajello, K. Murase, and A. McDaniel, (2023), arXiv:2307.02333 [astro-ph.HE].
- [34] K. Murase, S. S. Kimura, and P. Meszaros, *Phys. Rev. Lett.* **125**, 011101 (2020), arXiv:1904.04226 [astro-ph.HE].
- [35] A. Kheirandish, K. Murase, and S. S. Kimura, *Astrophys. J.* **922**, 45 (2021), arXiv:2102.04475 [astro-ph.HE].
- [36] B. Eichmann, F. Oikonomou, S. Salvatore, R.-J. Dettmar, and J. Becker Tjus, *Astrophys. J.* **939**, 43 (2022), arXiv:2207.00102 [astro-ph.HE].
- [37] Y. Inoue, D. Khangulyan, and A. Doi, *Astrophys. J. Lett.* **891**, L33 (2020), arXiv:1909.02239 [astro-ph.HE].
- [38] S. Inoue, M. Cerruti, K. Murase, and R.-Y. Liu, (2022), arXiv:2207.02097 [astro-ph.HE].
- [39] K. Murase, *Astrophys. J. Lett.* **941**, L17 (2022), arXiv:2211.04460 [astro-ph.HE].
- [40] C. Blanco, D. Hooper, T. Linden, and E. Pinetti, (2023), arXiv:2307.03259 [astro-ph.HE].
- [41] M. G. Aartsen *et al.* (IceCube, Fermi-LAT, MAGIC, AGILE, ASAS-SN, HAWC, H.E.S.S., INTEGRAL, Kanata, Kiso, Kapteyn, Liverpool Telescope, Subaru, Swift NuSTAR, VERITAS, VLA/17B-403), *Science* **361**, eaat1378 (2018), arXiv:1807.08816 [astro-ph.HE].
- [42] M. G. Aartsen *et al.* (IceCube), *Science* **361**, 147 (2018), arXiv:1807.08794 [astro-ph.HE].
- [43] S. Ansoldi *et al.* (MAGIC), *Astrophys. J. Lett.* **863**, L10 (2018), arXiv:1807.04300 [astro-ph.HE].
- [44] A. Keivani *et al.*, *Astrophys. J.* **864**, 84 (2018), arXiv:1807.04537 [astro-ph.HE].
- [45] P. Padovani, F. Oikonomou, M. Petropoulou, P. Giommi, and E. Resconi, *Monthly Notices of the Royal Astronomical Society: Letters* **484**, L104 (2019).
- [46] K. Murase, F. Oikonomou, and M. Petropoulou, As-

- trophys. J. **865**, 124 (2018), arXiv:1807.04748 [astro-ph.HE].
- [47] S. Gao, A. Fedynitch, W. Winter, and M. Pohl, *Nature Astron.* **3**, 88 (2019), arXiv:1807.04275 [astro-ph.HE].
- [48] M. Cerruti, A. Zech, C. Boisson, G. Emery, S. Inoue, and J.-P. Lenain, *Monthly Notices of the Royal Astronomical Society: Letters* **483**, L12 (2018).
- [49] B. T. Zhang, M. Petropoulou, K. Murase, and F. Oikonomou, *Astrophys. J.* **889**, 118 (2020), arXiv:1910.11464 [astro-ph.HE].
- [50] M. Petropoulou, K. Murase, M. Santander, S. Buson, A. Tohuvavohu, T. Kawamuro, G. Vasilopoulos, H. Negoro, Y. Ueda, M. H. Siegel, A. Keivani, N. Kawai, A. Mastichiadis, and S. Dimitrakoudis, *The Astrophysical Journal* **891**, 115 (2020).
- [51] A. Granelli, P. Ullio, and J.-W. Wang, *Journal of Cosmology and Astroparticle Physics* **2022**, 013 (2022).
- [52] S. Bhowmick, D. Ghosh, and D. Sachdeva, (2022), arXiv:2301.00209 [hep-ph].
- [53] E. D. Bloom and J. D. Wells, *Physical Review D* **57**, 1299 (1998).
- [54] M. Gorchtein, S. Profumo, and L. Ubaldi, *Physical Review D* **82** (2010), 10.1103/physrevd.82.083514.
- [55] D. Hooper and S. D. McDermott, *Phys. Rev. D* **97**, 115006 (2018), arXiv:1802.03025 [hep-ph].
- [56] C. V. Cappiello, K. C. Y. Ng, and J. F. Beacom, *Phys. Rev. D* **99**, 063004 (2019), arXiv:1810.07705 [hep-ph].
- [57] A. Ambrosone, M. Chianese, D. F. G. Fiorillo, A. Marinelli, and G. Miele, (2022), arXiv:2210.05685 [astro-ph.HE].
- [58] P. J. E. Peebles, *General Relativity and Gravitation* **3**, 63 (1972).
- [59] G. D. Quinlan, L. Hernquist, and S. Sigurdsson, *Astrophys. J.* **440**, 554 (1995), arXiv:astro-ph/9407005.
- [60] P. Gondolo and J. Silk, *Physical Review Letters* **83**, 1719 (1999).
- [61] P. Ullio, H. Zhao, and M. Kamionkowski, *Phys. Rev. D* **64**, 043504 (2001), arXiv:astro-ph/0101481.
- [62] F. Ferrer, A. M. da Rosa, and C. M. Will, *Phys. Rev. D* **96**, 083014 (2017), arXiv:1707.06302 [astro-ph.CO].
- [63] F. Ferrer, G. Herrera, and A. Ibarra, *JCAP* **05**, 057 (2023), arXiv:2209.06339 [hep-ph].
- [64] J. F. Navarro, C. S. Frenk, and S. D. M. White, *Astrophys. J.* **490**, 493 (1997), arXiv:astro-ph/9611107.
- [65] J. F. Navarro, C. S. Frenk, and S. D. M. White, *Astrophys. J.* **462**, 563 (1996), arXiv:astro-ph/9508025.
- [66] T. Lacroix, M. Karami, A. E. Broderick, J. Silk, and C. Boehm, *Physical Review D* **96** (2017), 10.1103/physrevd.96.063008.
- [67] T. Di Matteo, R. A. C. Croft, V. Springel, and L. Hernquist, *Astrophys. J.* **593**, 56 (2003), arXiv:astro-ph/0301586.
- [68] L. Ferrarese, *Astrophys. J.* **578**, 90 (2002), arXiv:astro-ph/0203469.
- [69] O. Piana, P. Dayal, M. Volonteri, and T. R. Choudhury, *Monthly Notices of the Royal Astronomical Society* **500**, 2146 (2020).
- [70] T. Lacroix, C. Boehm, and J. Silk, *Physical Review D* **92** (2015), 10.1103/physrevd.92.043510.
- [71] T. Lin, H.-B. Yu, and K. M. Zurek, *Phys. Rev. D* **85**, 063503 (2012), arXiv:1111.0293 [hep-ph].
- [72] R. Essig, E. Kuflik, S. D. McDermott, T. Volansky, and K. M. Zurek, *JHEP* **11**, 193 (2013), arXiv:1309.4091 [hep-ph].
- [73] M. Cirelli, N. Fornengo, B. J. Kavanagh, and E. Pinetti, *Phys. Rev. D* **103**, 063022 (2021), arXiv:2007.11493 [hep-ph].
- [74] K. Bondarenko, A. Boyarsky, T. Bringmann, M. Hufnagel, K. Schmidt-Hoberg, and A. Sokolenko, *JHEP* **03**, 118 (2020), arXiv:1909.08632 [hep-ph].
- [75] I. Angeli, *Atom. Data Nucl. Data Tabl.* **87**, 185 (2004).
- [76] A. Keivani, K. Murase, M. Petropoulou, D. B. Fox, S. B. Cenko, S. Chaty, A. Coleiro, J. J. DeLaunay, S. Dimitrakoudis, P. A. Evans, J. A. Kennea, F. E. Marshall, A. Mastichiadis, J. P. Osborne, M. Santander, A. Tohuvavohu, and C. F. Turley, *The Astrophysical Journal* **864**, 84 (2018).
- [77] A. H. Abdelhameed *et al.* (CRESST), *Phys. Rev. D* **100**, 102002 (2019), arXiv:1904.00498 [astro-ph.CO].
- [78] C. Amole *et al.* (PICO), *Phys. Rev. D* **93**, 052014 (2016), arXiv:1510.07754 [hep-ex].
- [79] L. Barak, I. M. Bloch, M. Cababie, G. Cancelo, L. Chaplinsky, F. Chierchie, M. Crisler, A. Drlica-Wagner, R. Essig, J. Estrada, E. Etzion, G. F. Moroni, D. Gift, S. Munagavalasa, A. Orly, D. Rodrigues, A. Singal, M. S. Haro, L. Stefanazzi, J. Tiffenberg, S. Uemura, T. Volansky, and T.-T. Y. and, *Physical Review Letters* **125** (2020), 10.1103/physrevlett.125.171802.
- [80] E. Aprile, J. Aalbers, F. Agostini, M. Alfonsi, L. Althueser, F. Amaro, V. Antochi, E. Angelino, F. Arneodo, D. Barge, L. Baudis, B. Bauermeister, L. Bellagamba, M. Benabderrahmane, T. Berger, P. Breur, A. Brown, E. Brown, S. Bruenner, G. Bruno, R. Budnik, C. Capelli, J. Cardoso, D. Cichon, D. Coderre, A. Colijn, J. Conrad, J. Cussonneau, M. Decowski, P. de Perio, A. Depoian, P. D. Gangi, A. D. Giovanni, S. Diglio, A. Elykov, G. Eurin, J. Fei, A. Ferella, A. Fieguth, W. Fulgione, P. Gaemers, A. G. Rosso, M. Galloway, F. Gao, M. Garbini, L. Grandi, Z. Greene, C. Hasterok, C. Hils, E. Hogenbirk, J. Howlett, M. Iacovacci, R. Itay, F. Joerg, S. Kazama, A. Kish, M. Kobayashi, G. Koltman, A. Kopec, H. Landsman, R. Lang, L. Levinson, Q. Lin, S. Lindemann, M. Lindner, F. Lombardi, J. Lopes, E. L. Fune, C. Macolino, J. Mahlstedt, A. Manfredini, F. Marignetti, T. M. Undagoitia, J. Masbou, S. Mastroianni, M. Messina, K. Micheneau, K. Miller, A. Molinario, K. Morã, Y. Mosbacher, M. Murra, J. Naganoma, K. Ni, U. Oberlack, K. Odgers, J. Palacio, B. Pelssers, R. Peres, J. Pienaar, V. Pizzella, G. Plante, R. Podviianiuk, J. Qin, H. Qiu, D. R. García, S. Reichard, B. Riedel, A. Rocchetti, N. Rupp, J. dos Santos, G. Sartorelli, N. Šarčević, M. Scheibelhut, S. Schindler, J. Schreiner, D. Schulte, M. Schumann, L. S. Lavina, M. Selvi, P. Shagin, E. Shockley, M. Silva, H. Simgen, C. Therreau, D. Thers, F. Toschi, G. Trinchero, C. Tunnell, N. Upole, M. Vargas, G. Volta, O. Wack, H. Wang, Y. Wei, C. Weinheimer, D. Wenz, C. Wittweg, J. Wulf, J. Ye, Y. Zhang, T. Zhu, and J. Z. and, *Physical Review Letters* **123** (2019), 10.1103/physrevlett.123.251801.
- [81] T. Emken, C. Kouvaris, and I. M. Shoemaker, *Phys. Rev. D* **96**, 015018 (2017), arXiv:1702.07750 [hep-ph].
- [82] T. Emken, R. Essig, C. Kouvaris, and M. Sholapurkar, *JCAP* **09**, 070 (2019), arXiv:1905.06348 [hep-ph].
- [83] M. S. Mahdawi and G. R. Farrar, *Journal of Cosmology and Astroparticle Physics* **2018**, 007 (2018).
- [84] M. A. Buen-Abad, R. Essig, D. McKeen, and Y.-M. Zhong, *Phys. Rept.* **961**, 1 (2022), arXiv:2107.12377

- [astro-ph.CO].
- [85] P. F. Depta, M. Hufnagel, K. Schmidt-Hoberg, and S. Wild, *Journal of Cosmology and Astroparticle Physics* **2019**, 029 (2019).
  - [86] C. Giovanetti, M. Lisanti, H. Liu, and J. T. Ruderman, *Phys. Rev. Lett.* **129**, 021302 (2022), arXiv:2109.03246 [hep-ph].
  - [87] H. An, M. Pospelov, J. Pradler, and A. Ritz, *Physical Review Letters* **120** (2018), 10.1103/physrevlett.120.141801.
  - [88] E. Kufflik, M. Perelstein, N. R.-L. Lorier, and Y.-D. Tsai, *Phys. Rev. Lett.* **116**, 221302 (2016), arXiv:1512.04545 [hep-ph].
  - [89] R. Essig, T. Volansky, and T.-T. Yu, *Physical Review D* **96** (2017), 10.1103/physrevd.96.043017.
  - [90] C. A. Argüelles, A. Kheirandish, and A. C. Vincent, *Physical Review Letters* **119** (2017), 10.1103/physrevlett.119.201801.
  - [91] K. J. Kelly and P. A. N. Machado, *JCAP* **10**, 048 (2018), arXiv:1808.02889 [hep-ph].
  - [92] K.-Y. Choi, J. Kim, and C. Rott, *Phys. Rev. D* **99**, 083018 (2019), arXiv:1903.03302 [astro-ph.CO].
  - [93] K. Murase and I. M. Shoemaker, *Physical Review Letters* **123** (2019), 10.1103/physrevlett.123.241102.
  - [94] J. Alvey and M. Fairbairn, *Journal of Cosmology and Astroparticle Physics* **2019**, 041 (2019).
  - [95] R. Eskenasy, A. Kheirandish, and K. Murase, *Phys. Rev. D* **107**, 103038 (2023), arXiv:2204.08924 [hep-ph].
  - [96] J. M. Cline, S. Gao, F. Guo, Z. Lin, S. Liu, M. Puel, P. Todd, and T. Xiao, (2022), arXiv:2209.02713 [hep-ph].
  - [97] J. M. Cline and M. Puel, (2023), arXiv:2301.08756 [hep-ph].
  - [98] Y. P. Jing and Y. Suto, *Astrophys. J. Lett.* **529**, L69 (2000), arXiv:astro-ph/9909478.
  - [99] D. Reed, F. Governato, L. Verde, J. Gardner, T. R. Quinn, J. Stadel, D. Merritt, and G. Lake, *Mon. Not. Roy. Astron. Soc.* **357**, 82 (2005), arXiv:astro-ph/0312544.
  - [100] D. Merritt, *Phys. Rev. Lett.* **92**, 201304 (2004), arXiv:astro-ph/0311594.
  - [101] O. Y. Gnedin and J. R. Primack, *Phys. Rev. Lett.* **93**, 061302 (2004), arXiv:astro-ph/0308385.
  - [102] D. Merritt, S. Harfst, and G. Bertone, *Phys. Rev. D* **75**, 043517 (2007), arXiv:astro-ph/0610425.
  - [103] T. Lacroix, *Astron. Astrophys.* **619**, A46 (2018), arXiv:1801.01308 [astro-ph.GA].
  - [104] Z.-Q. Shen, G.-W. Yuan, C.-Z. Jiang, Y.-L. S. Tsai, Q. Yuan, and Y.-Z. Fan, (2023), arXiv:2303.09284 [astro-ph.GA].
  - [105] M. H. Chan and C. M. Lee, *Astrophys. J. Lett.* **943**, L11 (2023), arXiv:2212.05664 [astro-ph.HE].
  - [106] A. Alachkar, J. Ellis, and M. Fairbairn, *Phys. Rev. D* **107**, 103033 (2023), arXiv:2207.10021 [hep-ph].



### Dependency of the constraints on the dark matter density profile

We have derived constraints on the dark matter-electron scattering cross section for different values of the pre-existing dark matter profile slope index. For the purpose of concreteness, we consider NFW-like profiles with slope indices in the range  $\gamma = 0.05 - 2$ , to assess the conclusions of our work beyond the benchmark case covered in the main text,  $\gamma = 1$ . We normalize all profiles such that the total mass of the dark matter halo of TXS 0506+056 is bound by  $M_{\text{DM}} \lesssim 10^{13} M_{\odot}$ . In the left panel of Fig. 4, we show the dark matter profiles in the vicinity of TXS 0506+056 for different values of  $\gamma$ . As expected, the dark matter density profile becomes steeper for larger values of  $\gamma$ , and the size of the spike becomes smaller. Outside the spike, the profiles initially evolve with power  $\rho_{\text{DM}} \propto r^{-3+\gamma}$ , but sufficiently far from the center they converge to a  $\rho_{\text{DM}} \propto r^{-\gamma}$  behaviour. On the right panel of the figure, we show the upper limits on the dark matter-electron scattering cross section found for those profiles corresponding to asymmetric (or slowly annihilating) dark matter. As can be noticed in the figure, the constraints can vary 5 to 6 orders of magnitude depending on the value of  $\gamma$ , although only vary within 1 order of magnitude in the range  $\gamma = 0.6 - 1.4$ , which is favoured by some simulations of Milky Way analogues [98, 99].

However, shallower profiles might arise *e.g.*, due to gravitational scattering of dark matter with stars [100, 101], with  $\gamma_{\text{sp}} = 1.5$ , or due to mergers of galaxies [102], among other possibilities. Dynamical constraints on the existence of spikes have been derived for some sources, with inconclusive results so far, but certainly disfavouring spikes formed from NFW profiles with  $\gamma > 1$  *à la Gondolo and Silk* [103–106].

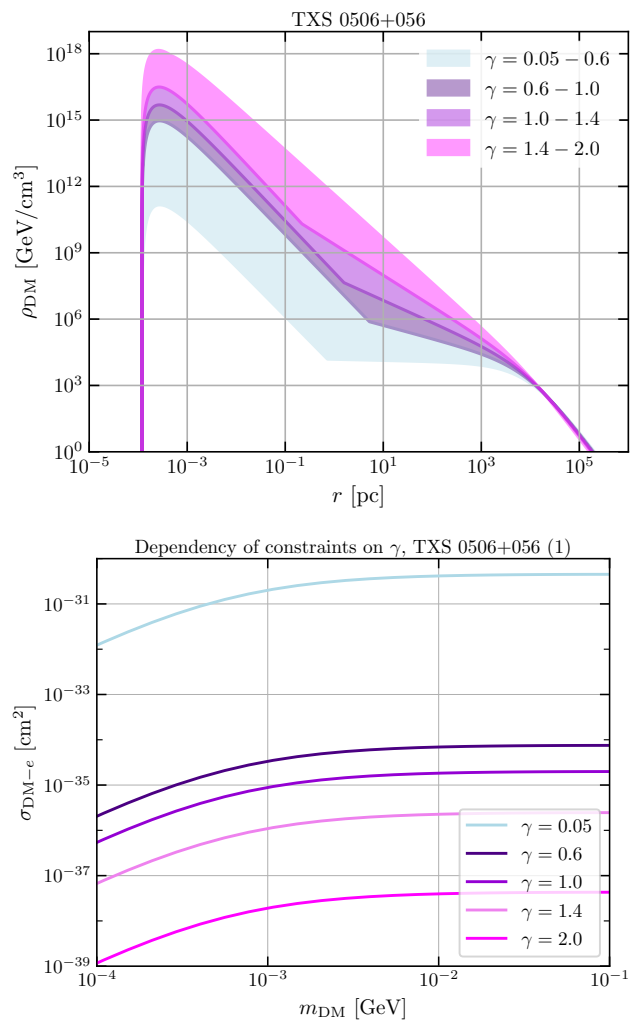


FIG. 4. *Upper panel:* Dark matter distribution around the black hole of TXS 0506+056, for different values of the pre-existing dark matter profile slope  $\gamma$ . *Lower panel:* Upper limits on the sub-GeV dark matter-proton scattering cross section over the dark matter mass from TXS 0506+056, for different values of the index  $\gamma$ .